THE JOURNAL OF BIOLOGICAL CHEMISTRY
Vol. 278, No. 11, Issue of March 14, pp. 9928–9937, 2003
Printed in U.S.A.

A Novel Fluorescent Toxin to Detect and Investigate Kv1.3 Channel Up-regulation in Chronically Activated T Lymphocytes*

Received for publication, December 18, 2002, and in revised form, January 1, 2003
Published, JBC Papers in Press, January 2, 2003, DOI 10.1074/jbc.M212868200

Christine Beeton‡, Heike Wulff‡, Satendra Singh§, Steve Botsko§, George Crossley§, George A. Gutman‡¶, Michael D. Cahalan‡, Michael Pennington§, and K. George Chandy‡‖

From the ‡Department of Physiology and Biophysics, University of California, Irvine, California 92697, §Bachem Bioscience, King of Prussia, Pennsylvania 19406, and the ¶Department of Microbiology and Molecular Genetics, University of California, Irvine, California 92697

T lymphocytes with unusually high expression of the voltage-gated Kv1.3 channel (Kv1.3^{high} cells) have been implicated in the pathogenesis of experimental autoimmune encephalomyelitis, an animal model for multiple sclerosis. We have developed a fluoresceinated analog of ShK (ShK-F6CA), the most potent known inhibitor of Kv1.3, for detection of Kv1.3^{high} cells by flow cytometry. ShK-F6CA blocked Kv1.3 at picomolar concentrations with a Hill coefficient of 1 and exhibited >80-fold specificity for Kv1.3 over Kv1.1 and other K_V channels. In flow cytometry experiments, ShK-F6CA specifically stained Kv1.3-expressing cells with a detection limit of ~600 channels per cell. Rat and human T cells that had been repeatedly stimulated 7–10 times with antigen were readily distinguished on the basis of their high levels of Kv1.3 channels (>600 channels/cell) and ShK-F6CA staining from resting T cells or cells that had undergone 1–3 rounds of activation. Functional Kv1.3 expression levels increased substantially in a myelin-specific rat T cell line following myelin antigen stimulation, peaking at 15–20 h and then declining to baseline over the next 7 days, in parallel with the acquisition and loss of encephalitogenicity. Both calcium- and protein kinase C-dependent pathways were required for the antigen-induced Kv1.3 up-regulation. ShK-F6CA might be useful for rapid and quantitative detection of Kv1.3^{high} expressing cells in normal and diseased tissues, and to visualize the distribution of functional channels in intact cells.

Human T lymphocytes express two potassium channels, the voltage-gated K^+ channel *Kv1.3* and the calcium-activated K^+ channel *IKCa1,* that are involved in proliferation and cytokine secretion (1–6). Recently, we reported (7) that myelin-reactive encephalitogenic rat T cells expressed unusually high numbers of Kv1.3 channels following eight or more repeated antigenic stimulations *in vitro*. Adoptive transfer of these Kv1.3^{high} T cells into rats induced experimental autoimmune encephalomyelitis (EAE).[1] EAE is an animal model for multiple sclerosis (MS), a chronic inflammatory disease of the central nervous system characterized by immune-mediated focal demyelination and axonal damage resulting in severe neurological deficits (8–10). Studies with several myelin-specific rat T cell lines revealed a correlation between encephalitogenicity and the number of expressed Kv1.3 channels (7, 11). In addition, *in vivo* Kv1.3 blockade ameliorated adoptive EAE, suggesting a crucial role of Kv1.3 in the pathogenicity of these cells (7, 12). A rapid method to detect Kv1.3^{high} lymphocytes might therefore facilitate studies of the role of Kv1.3 in the pathogenesis of MS and its potential as a therapeutic target for this disease.

The patch clamp technique is widely used to determine functional *Kv1.3* and *IKCa1* channel levels in lymphocytes but requires highly specialized equipment and is time-consuming, allowing the study of only a few dozen cells per day. Reverse transcriptase-PCR and Western blot analysis provide a measure of channel-transcript or channel-protein expression in lymphocytes but not the number of functional channels in the cell membrane. All known Kv1.3-specific antibodies target intracellular epitopes (13) in the channel making it necessary to permeabilize lymphocytes before they can be stained with these reagents. In addition, nonspecific staining imposes a further limitation to the use of antibodies for protein detection. Furthermore, no reports have yet described any success in using these antibodies for immunostaining lymphocytes, necessitating the development of novel tools to identify Kv1.3^{high} lymphocytes in tissues.

Despite the clear need for fluorescently labeled toxins as markers of channel expression and distribution in intact cells, there have been only a few reports of channel-binding peptides that have been successfully tagged with fluorophores. Fluorophore-labeled channel-binding peptides were reported previously for sodium channels (14, 15), voltage-activated calcium channels (16), and *N*-methyl-D-aspartic acid receptors (17). Most recently, a fluorophore-tagged hongotoxin analog was used to detect Kv1.1 and Kv1.2 channels in rat brain sections and Kv1.3 in Jurkat cells (18, 19). Several Kv1.3-blocking polypeptides have been discovered by us and by others (5, 20–24) in scorpion venom and sea anemone extracts. Because these polypeptides bind with extremely high affinities to Kv1.3, they might be used in much the same way as antibodies. Unlike

* This work was supported by grants from the National Multiple Sclerosis Society (to K. G. C.), National Institutes of Health Grants MH59222 and NS14609, and a postdoctoral fellowship from the National Multiple Sclerosis Society (to C. B.). The costs of publication of this article were defrayed in part by the payment of page charges. This article must therefore be hereby marked "*advertisement*" in accordance with 18 U.S.C. Section 1734 solely to indicate this fact.

‖ To whom correspondence should be addressed: Rm. 291, Joan Irvine Smith Hall, University of California Medical School, Irvine, CA 92697. Tel.: 949-824-2133; Fax: 949-824-3143; E-mail: gchandy@uci.edu.

[1] The abbreviations used are: EAE, experimental autoimmune encephalomyelitis; Aeea, aminoethyloxyethyloxy-acetyl; APC, antigen-presenting cell; ChTX, charybdotoxin; Con A, concanavalin A; CsA, cyclosporin A; F6CA, fluorescein-6-carboxyl; MBP, myelin basic protein; MgTX, margatoxin; MS, multiple sclerosis; PBMC, peripheral blood mononuclear cells; PKC, protein kinase C; ShK, *Stichodactyla helianthus* toxin; TCGF, T cell growth factor; TEA, tetraethylammonium; TMR, tetramethylrhodamine; TT, tetanus toxoid; FCS, fetal calf serum; Fmoc, *N*-(9-fluorenyl)methoxycarbonyl; Ab, antibody; Pmc, 2,2,5,7,8-pentamethylchroman-6-sulfonyl-; Trt, triphenylmethyl-; *t*Bu, *tert*-butyl-; Boc, *tert*-butyloxycarbonyl-; HOBT, 1-hydroxybenzotriazole.

Kv1.3-specific antibodies, these polypeptides bind to the outer vestibule of Kv1.3 and can therefore reach their binding pocket in live intact lymphocytes. ShK, a 35-amino acid polypeptide from the Caribbean sea anemone *Stichodactyla helianthus,* is the most potent known inhibitor of Kv1.3 (K_d 11 pM), and once bound to the channel does not wash off easily (5). ShK binds via high affinity interactions to residues in the outer vestibule of the channel (5, 25). If suitably tagged with fluorophores, ShK could be used as a molecular probe to detect Kv1.3^{high} lymphocytes by flow cytometry.

In this study, guided by the high resolution structure of ShK (26, 27) and the experimentally verified ShK-Kv1.3-interacting surface (5, 25, 28), we attached fluorescein-6- carboxyl (F6CA) through an aminoethyloxyethyloxy-acetyl (Aeea) linker to the α-amino group of Arg^1. This residue was chosen because it is located on the back side of the toxin surface facing away from the channel pore. We chose the 11-carbon atom linker Aeea to minimize steric effects caused by the aromatic moiety of F6CA in binding and folding of the peptide. The labeled polypeptide selectively blocked Kv1.3 with picomolar affinity. In flow cytometry experiments, chronically activated rat and human T lymphocytes with >600 Kv1.3 channels/cell were detected by ShK-F6CA staining, whereas resting and acutely activated lymphocytes with lower Kv1.3 channel numbers were not visualized by this method. ShK-F6CA may therefore be a useful tool to detect the presence of Kv1.3^{high} lymphocytes under normal and diseased conditions.

EXPERIMENTAL PROCEDURES

Reagents—Guinea pig myelin basic protein (MBP), concanavalin A (Con A), cyclosporin A (CsA), and staurosporine were from Sigma. *S. helianthus* toxin (ShK), margatoxin (MgTX), charybdotoxin (ChTX), and apamin were from Bachem (King of Prussia, PA). Tetanus toxoid (TT) was a generous gift from Dr. Peter A. Calabresi (University of Maryland).

Generation of the ShK Conjugates—Fmoc-amino acids (Bachem A.G., CH-4416 Bubendorf, Switzerland) included the following: Ala, Arg-(Pmc), Asn(Trt), Asp(OtBu), Cys(Trt), Gln(Trt), Glu(OtBu), Gly, His-(Trt), Ile, Leu, Lys(Boc), Met, Phe, Pro, Ser(*t*Bu), Thr(*t*Bu), and Tyr(*t*Bu). Stepwise assembly was carried out starting with 10 g of Fmoc-Cys(Trt)-resin (0.65 mmol/g) on a Labortec SP4000 peptide synthesizer. Following final removal of the Fmoc-group from the N-terminal Arg residue, a resin aliquot was removed, and the hydrophilic linker Fmoc-Aeea-OH (Fmoc-amino-ethyloxy-ethyloxyacetic acid) was coupled as an HOBT ester. This resin was subsequently divided into four portions for preparation of the biotinyl (for ShK-biotin), fluorescein-6-carboxyl (for ShK-F6CA), tetramethylrhodamine-6-carboxyl (for ShK-TMR), or the biotinyl-$(Aeea)_4$ derivatives. Each of these residues was also coupled as an HOBT ester after deblocking the Fmoc group. Following N-terminal derivatization, each of the peptides was cleaved from the resin and simultaneously deprotected with reagent K (29) for 2 h at room temperature. The free peptide was then filtered to remove the spent resin beads and precipitated with ice-cold diethyl ether, collected on a fine filter by suction, washed with ice-cold ether, and finally extracted with 20% AcOH in H_2O. Oxidative folding of the disulfide bonds and its subsequent purification were as described previously (23) with the addition of 25% MeOH to the solution to maintain solubility. Oxidative folding was facilitated by addition of 1.5 mM reduced glutathione and 0.75 mM oxidized glutathione. Each sample was purified by preparative reverse phase-high pressure liquid chromatography using a Rainin Dynamax C18 column. High pressure liquid chromatography-pure fractions for each sample were pooled and lyophilized. Structures and purity of all analogs were confirmed by high pressure liquid chromatography and amino acid and matrix-assisted laser desorption ionization/time of flight analysis.

Cells—L929, B82, and MEL cells stably expressing *mKv1.1*, *rKv1.2*, *mKv1.3*, *mKv3.1*, and *hKv1.5* have been described previously (30) and were maintained in Dulbecco's modified Eagle's medium containing 10% heat-inactivated FCS (Summit Biotechnology, Fort Collins, CO), 4 mM L-glutamine, 1 mM sodium pyruvate, and 500 μg/ml G418 (Calbiochem). LTK cells expressing *hKv1.4* were obtained from M. Tamkun (University of Colorado, Boulder). An enhanced green fluorescent protein-C3 construct containing *mKv1.7* (31) was transiently transfected into COS-7 cells using FuGENE 6 (Roche Molecular Biochemicals) according to the manufacturer's protocol. Kv1.7 currents were recorded 6–8 h after transfection.

The PAS T cell line was a kind gift from Dr. Evelyne Béraud (Marseille, France). This long term cell line, specific for MBP, was generated in Lewis rats and expresses only two types of K^+ channels, Kv1.3 and IKCa1 (7). Once activated with MBP and injected into naive Lewis rats, PAS T cells induce EAE (7, 12, 32). They were maintained in culture by alternating rounds of antigen-induced activation and rounds of expansion in interleukin-2-containing medium. For antigen stimulation, PAS T cells (3×10^5/ml) were incubated for 2 days with 10 μg/ml MBP and 15×10^6/ml syngeneic irradiated (2500 rads) thymocytes as antigen-presenting cells (APCs) in RPMI 1640 Dutch modification containing 4 mM glutamine, 1 mM sodium pyruvate, 1% nonessential amino acids, 1% RPMI vitamins, 100 units/ml penicillin, 100 μg/ml streptomycin, and 50 μM β-mercaptoethanol (basic medium) supplemented with 1% syngeneic rat serum. For the interleukin-2-dependent growth phase, PAS cells were seeded in basic medium supplemented with 10% FCS and 5% T cell growth factor (TCGF). After 5 days of expansion in this medium, PAS T cells were restimulated with MBP. TCGF was produced by activating Lewis rat (5–8 weeks old; Charles

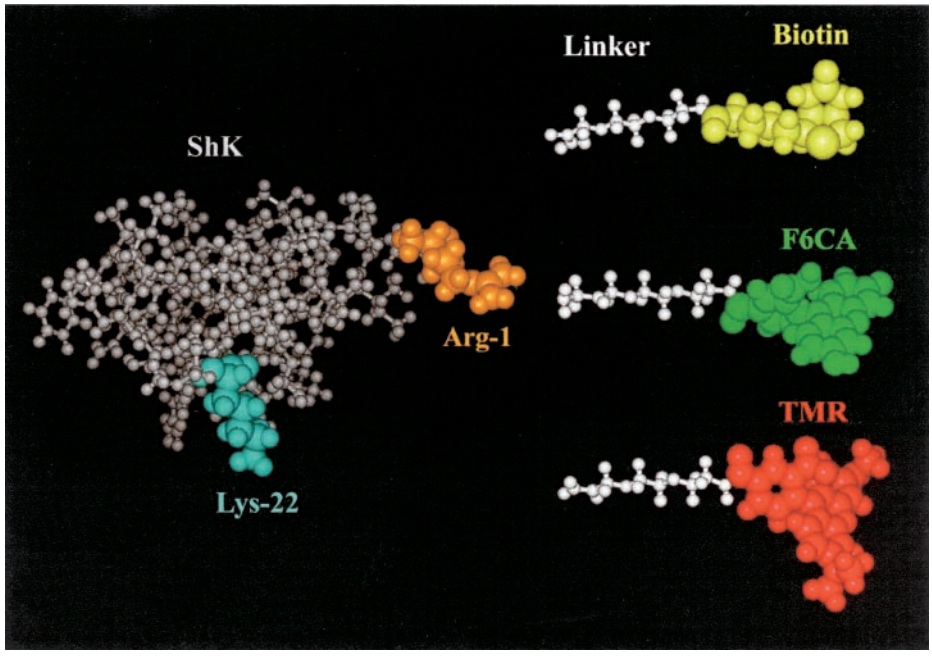

FIG. 1. **Generation of ShK conjugates.** F6CA (highlighted in *green*), biotin (highlighted in *yellow*), or TMR (highlighted in *red*) were conjugated to ShK (*left*) through a linker attached on its N terminus (residue Arg^1, in *orange*). The Lys^{22}, required for channel blockade, is highlighted in *cyan.* The molecular model of ShK is based on the published NMR structure (5, 26); the structures of F6CA-, biotin-, and TMR-Aeea were modeled with AM1 in Hyperchem.

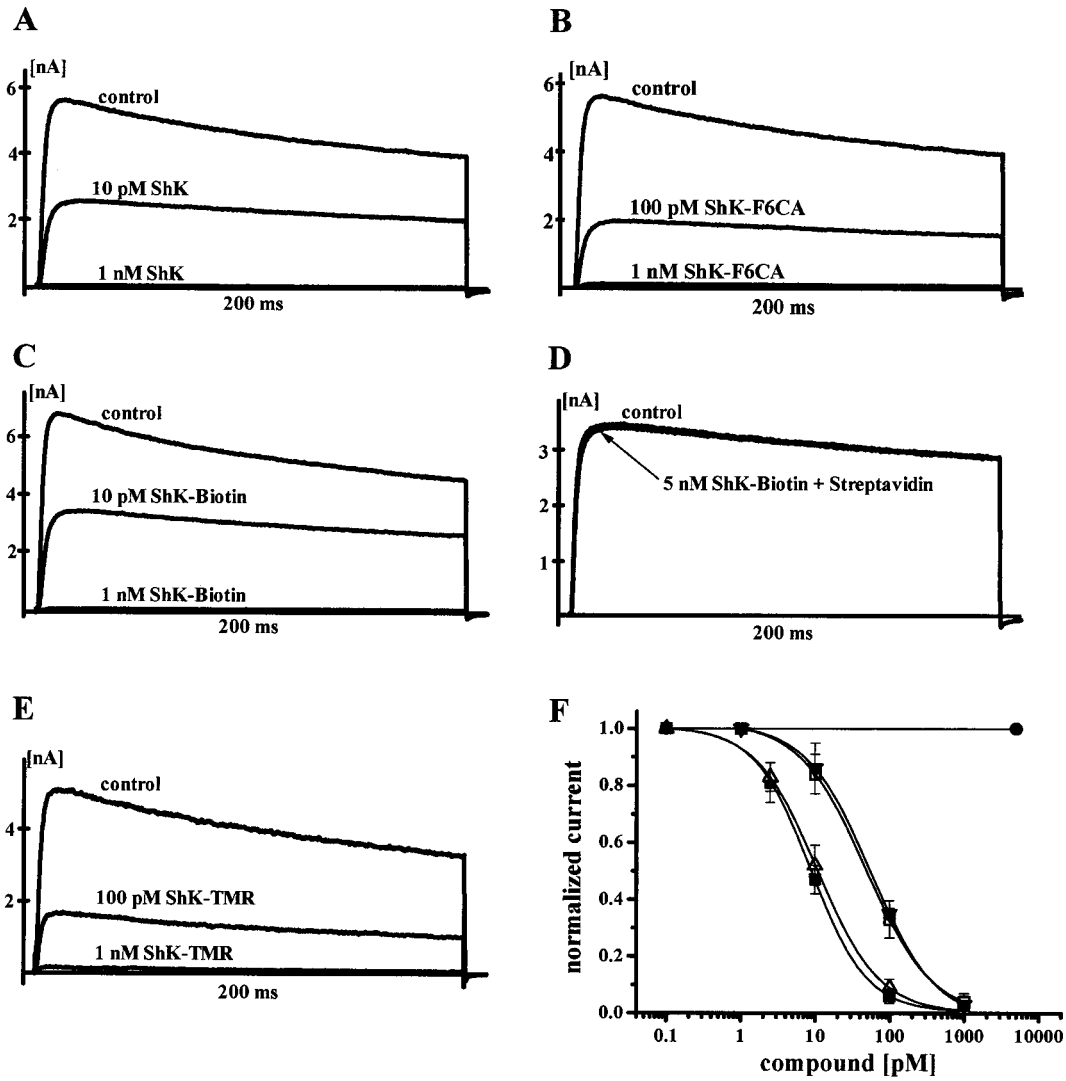

FIG. 2. **ShK conjugates block Kv1.3 channels at picomolar concentrations.** Effect of ShK (*A*), ShK-F6CA (*B*), ShK-biotin alone (*C*), or preincubated with streptavidin (*D*), and ShK-TMR (*E*) on Kv1.3 currents in stably transfected L929 cells. *F*, dose-dependent inhibition of Kv1.3 currents by ShK (■, K_d = 10 ± 1 pM, n_H = 1.15), ShK-F6CA (□, K_d = 48 ± 4 pM, n_H = 0.98), ShK-biotin (△, K_d = 11 ± 2 pM, n_H = 1.05), ShK-biotin preincubated with streptavidin (●), and ShK-TMR (▼, K_d = 52 ± 5 pM, n_H = 0.99). Each data point is the mean of three determinations.

River Laboratories, Wilmington, MA) splenocytes (2×10^6/ml) with 2 μg/ml Con A in basic medium supplemented with 10% FCS. After 48 h cells were pelleted, and 15 mg/ml α-methylmannoside (Sigma) was added to the supernatant to inactivate Con A. After thorough mixing the supernatant was passed through a 0.2-μm filter and stored at −20 °C.

Rat and human mononuclear cells were isolated from the spleens of Lewis rats or from the blood of healthy volunteers, and enriched for T cells by nylon wool purification for rat T cells or with $CD3^+$ RosetteSep (StemCell Technologies, Vancouver, British Columbia, Canada) for human T cells. Rat T cells were activated with 5 μg/ml Con A; human T cells were activated with 50 ng/ml anti-CD3 Ab (Biomeda) in the presence of autologous irradiated (2500 rads) peripheral blood mononuclear cells (PBMC) as APCs for 48 h. Human TT or MBP-specific T cells were generated from PBMCs from a healthy volunteer. Cells (2×10^8) were stimulated with 10 μg/ml TT or MBP. After 2 days 5% TCGF was added, and the cells were expanded for 5 days. Cells were restimulated in regular 7-day cycles with TT or MBP in the presence of autologous irradiated PBMCs. Experiments were performed after the 9th stimulation when 95% of cells expressed an effector memory phenotype.

Electrophysiological Analysis—All experiments were carried out in the whole-cell configuration of the patch clamp technique with a holding potential of −80 mV. Pipette resistances averaged 1.5 megohms, and series resistance compensation of 80% was employed when currents exceeded 2 nA. Kv1.3 currents were elicited by repeated 200-ms pulses from −80 to 40 mV, applied every 30 s. Kv1.3 currents were recorded in normal Ringer solution with a calcium-free pipette solution containing (in mM): 145 KF, 10 HEPES, 10 EGTA, 2 $MgCl_2$, pH 7.2, 300 mOsm. Whole-cell conductances were calculated from the peak current amplitudes at 40 mV, and Kv1.3 channel numbers per cell were calculated by dividing the whole-cell conductance by the single-channel conductance (12 pS). Kv1.1, Kv1.2, Kv1.4, Kv1.5, Kv1.7, Kv3.1 and IKCa1 currents were measured as described previously (7, 30, 31, 33).

Cell Staining with ShK Conjugates and Flow Cytometry Analysis—Adherent L929 (Kv1.1 and Kv1.3), B82 (Kv1.2), and LTK (Kv1.4) cells were detached from culture flasks with trypsin-EDTA. Detached cells or suspension cells (lymphocytes or MEL cells expressing Kv1.5) were washed twice with PBS and incubated in the dark at room temperature with 10 nM ShK-conjugate in PBS + 2% goat serum (Sigma) for 30 min and then washed 3× with PBS + 2% goat serum before flow cytometry analysis. For ShK-biotin and ShK-$(Aeea)_4$-biotin staining, this primary step was followed by a 30-min incubation with 2 μg/ml streptavidin-phycoerythrin (Pharmingen) or streptavidin-Alexa Fluor 488 (Molecular Probes) and 3 washes with PBS + 2% goat serum. For competition experiments cells were preincubated with 100 nM unlabeled ShK, 1 μM MgTX, 1 μM ChTX, or 5 μM apamin before addition of 10 nM ShK-F6CA. Stained cells were analyzed by flow cytometry on a BD Biosciences FACScan. Data were further analyzed using CellQuest software.

Pharmacological Analysis of the Pathways Involved in the Up-regulation of Kv1.3 Channels—Rested PAS T cells were incubated with 100 nM CsA, 10 nM staurosporine, or 100 nM MgTX for 1 h. MBP and APCs were added for a further 20–30 h to activate the cells before patch clamp and flow cytometry analysis (see above). Statistical analysis was carried out using the non-parametric Mann-Whitney *U* test.

RESULTS

ShK-F6CA, ShK-Biotin, and ShK-TMR Are Potent Kv1.3 Inhibitors—By using the polypeptide ShK as a template, we generated a novel fluoresceinated peptide toxin for use in flow cytometry to rapidly detect T cells that exhibit high levels of Kv1.3 channels. The parent peptide toxin ShK blocks Kv1.3 with picomolar affinity by binding to the outer vestibule of the channel, one polypeptide molecule per Kv1.3 tetramer (5, 25). ShK was first assembled stepwise through solid phase synthesis (23). After removal of a protecting group, Arg^1 of ShK was reacted with the hydrophilic linker Aeea and then coupled through this linker with F6CA (ShK-F6CA), biotin (ShK-biotin), or tetramethylrhodamine (ShK-TMR). The respective ShK-derivatives were cleaved from the resin and folded as described previously (23).

The NMR structure of ShK (26) and the AM-1 modeled structures of Aeea-F6CA, Aeea-biotin, and Aeea-TMR are shown in Fig. 1. ShK-Arg^1, the residue of which these linkers are attached (highlighted in *orange*) is on the "back side" of ShK (5, 25, 28). Lys^{22}, the critical residue on the channel-binding surface of ShK that occludes the Kv1.3 channel pore (5, 25, 28), is highlighted in *cyan*. The fluorophores were attached to Arg^1 in order to minimize the likelihood of interference with the interaction of polypeptide with the channel. Our strategy of labeling ShK during synthesis avoided the possibility of accidental labeling the crucial ϵ-amino group of Lys^{22}.

ShK-F6CA, ShK-biotin, ShK-TMR, and native ShK were tested for their ability to block mouse Kv1.3 channels stably expressed in L929 cells. Kv1.3 currents were elicited by 200-ms depolarizing steps from a holding potential of −80 mV to 40 mV (Fig. 2, *A–E*). Native ShK blocked these currents at picomolar concentrations (Fig. 2*A*), and the dose-response curve shown in Fig. 2*F* revealed a K_d of 10 pM. ShK-F6CA (K_d = 48 ± 4 pM) and ShK-TMR (52 ± 5 pM) were 4-fold less potent than ShK (Fig. 2, *B*, *E*, and *F*). Although the affinity of ShK-biotin for Kv1.3 (K_d = 11 ± 2 pM) was comparable with that of ShK, it was completely ineffective when pre-assembled with phycoerythrin-conjugated streptavidin (Fig. 2, *C*, *D*, and *F*), probably because the complex was too large to reach the binding site in the channel pore. Attachment of biotin via a longer linker (33 Å in length) to ShK dramatically reduced its affinity for Kv1.3 (K_d >100 nM; not shown in graph). All these polypeptides blocked Kv1.3 with a Hill coefficient of 1. These results demonstrate that ShK retains its ability to block the Kv1.3 channel at picomolar concentrations after the attachment of a fluorophore to Arg^1.

ShK-F6CA Is a Specific Inhibitor of Kv1.3 Channels—ShK is reported to block Kv1.3 and the neuronal channel Kv1.1 with equivalent potency (5). We therefore examined the ability of ShK-F6CA, ShK-TMR, ShK-biotin, and native ShK to block mouse Kv1.1 channels stably expressed in L929 cells. We used the classical K^+ channel blocker, TEA as a control, because Kv1.1 is one of the most TEA-sensitive channels. As expected, Kv1.1 was potently blocked by ShK (K_d = 25 ± 3 pM) (Fig. 3*A*) and exhibited low micromolar sensitivity to TEA (Fig. 3*B*). Surprisingly, ShK-F6CA was 160-fold less effective (K_d = 4.0 ± 0.3 nM) than ShK (Fig. 3*A*) and showed 83-fold greater affinity for Kv1.3 over Kv1.1 (compare Fig. 2, *A* and *F,* with Fig. 3*A*). In contrast, ShK-TMR and ShK-biotin blocked Kv1.1 at picomolar concentrations (ShK-TMR, K_d = 397 ± 36 pM; ShK-biotin, K_d = 114 ± 8 pM) and only exhibited 7–10-fold higher affinity for Kv1.3 than Kv1.1 (compare Fig. 2*F* and Fig. 3, *B* and *C*). The enhanced specificity of ShK-F6CA for Kv1.3 over Kv1.1 might be explained by the differences in charge of F6CA, TMR, and biotin: F6CA is negatively charged; TMR is positively charged; and biotin is neutral. In a recent experimentally determined

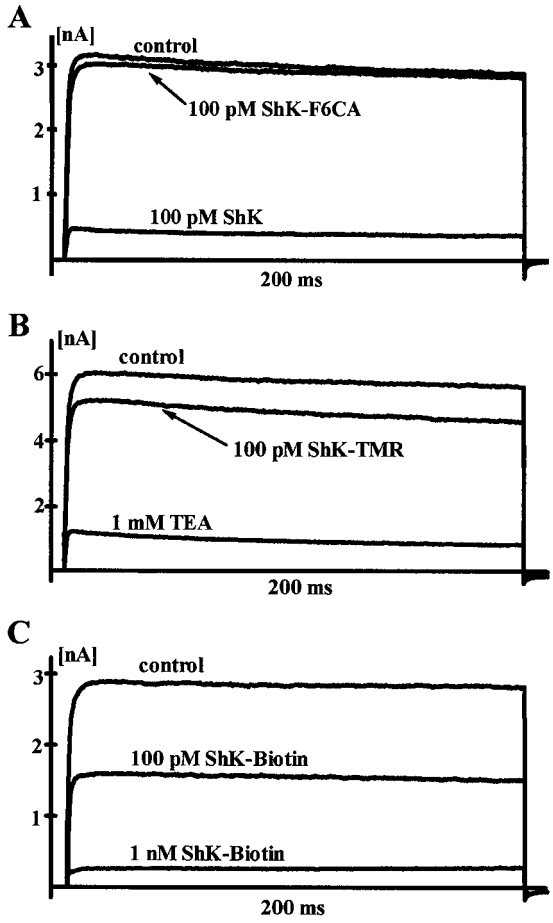

FIG. 3. **Conjugating ShK to F6CA, but not to TMR or biotin, reduces its affinity for Kv1.1 channels.** Kv1.1 currents were elicited by 200-ms depolarizing steps from a holding potential of −80 to 40 mV. Effect of ShK and ShK-F6CA (*A*), ShK-TMR and TEA (*B*), and ShK-biotin (*C*) on Kv1.1 currents is expressed by stably transfected cells.

docking configuration of ShK in the Kv1.3 vestibule (28), ShK-Arg^1 was found to be in the vicinity of Asp^{376}-Asp^{377}-Pro^{377}-Ser^{378}-Ser^{379} on the channel. If ShK sits in the Kv1.1 vestibule with the same geometry as it does in Kv1.3, the presence of three glutamates in the corresponding sequence in Kv1.1 (Glu^{350}-Glu^{351}-Ala^{352}-Glu^{353}-Ser^{354}) could electrostatically repel the negatively charged F6CA, while not affecting ShK-biotin and possibly strengthening the interaction with ShK-TMR. Negatively charged channel residues in neighboring loops (*e.g.* S3–S4 and S1–S2) may also contribute to the diminished potency of ShK-F6CA for Kv1.1.

We further tested the specificity of ShK-F6CA for Kv1.3 by screening it against a panel of additional K_V channels that were either stably expressed in mammalian cells (mKv1.2, hKv1.4, hKv1.5, and mKv3.1) or transiently transfected (mKv1.7). ShK-F6CA, like ShK, did not block mKv1.2, hKv1.5, mKv1.7, and mKv3.1 at concentrations up to 100 nM (Table I) as expected from published reports (5). Surprisingly, neither peptide blocked human Kv1.4 (Table I), although mouse Kv1.4, transiently expressed in *Xenopus* oocytes, has been reported to be blocked in the mid-picomolar range by ShK (5). The reason for this difference in results is not clear. Collectively, our data indicate that ShK-F6CA, but not ShK-TMR or ShK-biotin, is a specific inhibitor of Kv1.3 channels.

ShK-F6CA Staining and Flow Cytometry Detects Kv1.3 Channels in Mammalian Cells—ShK-F6CA stained L929 cells stably expressing roughly 2000 Kv1.3 channels/cell, the fluorescence signal in these cells being clearly distinguishable from

TABLE I
Selectivity of ShK, ShK-F6CA, ShK-TMR, and ShK-biotin on K_V channels

The K_d values from three independent determinations are given in pM ± S.D. Statistical analysis was carried out using the analysis of variance test.

Channel	ShK	ShK-F6CA	ShK-TMR	ShK-biotin
Kv1.1	25 ± 3	4,000 ± 300	397 ± 36	114 ± 8
		$p < 0.001$	$p < 0.001$	$p < 0.001$
Kv1.2	>100,000	>100,000		
Kv1.3	10 ± 1	48 ± 4	52 ± 5	11 ± 2
		$p < 0.001$	$p < 0.001$	$p > 0.05$
Kv1.4	>100,000	>100,000		
Kv1.5	>100,000	>100,000		
Kv1.7	>100,000	>100,000		
Kv3.1	>100,000	>100,000		

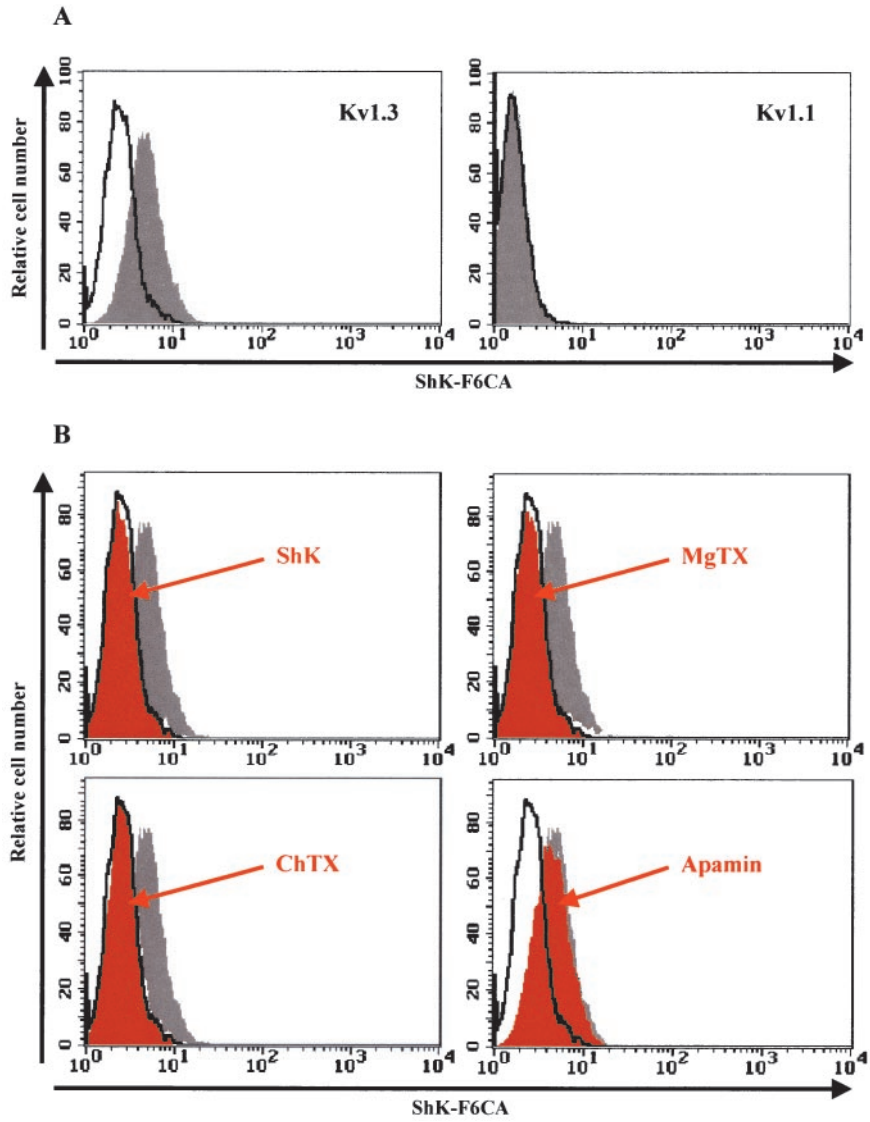

FIG. 4. **ShK-F6CA specifically stains cells expressing Kv1.3 channels.** *A*, flow cytometry profiles of cells stably expressing Kv1.3 (*left*) or Kv1.1 channels (*right*) unstained (*black line*) or stained with 10 nM ShK-F6CA (*shaded*). *B*, competition of ShK-F6CA staining with 100 nM unlabeled ShK, 1 μM MgTX, 1 μM ChTX, or 5 μM apamin (*red filled*). Control unstained cells are shown with *black lines*; cells stained with 10 nM ShK-F6CA are shown as the *shaded region*, and competitions are shown in *red*.

that in unstained cells (Fig. 4*A*, *left*). The addition of an anti-fluorescein Ab conjugated to Alexa-488 (Molecular Probes) did not increase the intensity of the stain, probably because the size of the Ab prevented it from reaching ShK-F6CA docked in the channel vestibule (data not shown). ShK-TMR also stained these cells although less brightly (data not shown), possibly because TMR is a less bright fluorophore with a lower quantum yield than F6CA. An excess of unlabeled Kv1.3 inhibitors (ShK, MgTX, and ChTX) competitively inhibited ShK-F6CA staining, whereas an inhibitor of small-conductance calcium-activated K^+ channels (apamin) had no effect (Fig. 4*B*). The specificity of ShK-F6CA for cells with Kv1.3 channels was further confirmed by the lack of staining of L929 cells stably expressing an equivalent number of Kv1.1 (Fig. 4*A*, *right*) or Kv3.1 (not shown) channels.

Identification of Kv1.3^{high} T Cells by ShK-F6CA Staining—Our success in identifying Kv1.3-bearing cells by ShK-F6CA staining and flow cytometry encouraged us to screen rat and human lymphocytes for Kv1.3 expression. Fig. 5 shows Kv1.3 currents and flow cytometry profiles of ShK-F6CA staining in rat (*left panel*) and human (*right*) T lymphocytes. Rat T lymphocytes freshly isolated from spleen contained barely detect-

able Kv1.3 currents, corresponding to about 5 Kv1.3 channels/cell. The Kv1.3 current amplitude increased 48 h after activation with the mitogen Con A (5 μg/ml), averaging about 200–300 channels/cell (Fig. 5, *middle left panels*). Neither resting nor activated rat T cells showed detectable ShK-F6CA staining, presumably because the Kv1.3 channel number in these cells is below the level of detection. In contrast, chronically stimulated MBP-reactive encephalitogenic rat T cells (7, 12, 32) exhibit, after activation, large Kv1.3 currents (~2000 channels/cell) and small IKCa1 currents (~100 channels/cell) and are brightly stained by ShK-F6CA (Fig. 5, *left bottom panels*) 48 h after the last antigenic stimulation. Upon stimulation, rat T lymphocytes preferentially up-regulate either IKCa1 or Kv1.3 channels depending on the number of encounters with antigen (7). The first three stimulations induce an up-regulation of IKCa1 channels, but if the cells undergo more rounds of stimulation (seven or more), they down-regulate IKCa1 and up-regulate Kv1.3 channels. ShK-F6CA therefore only stains activated T cells that have been repeatedly stimulated and rely preferentially on Kv1.3 channels for their proliferation.

We extended these findings to human T lymphocytes that correspond to the three groups of cells examined in rats. Freshly isolated unstimulated peripheral blood T lymphocytes expressed about 300–400 channels per cell and did not stain with ShK-F6CA (Fig. 5, *top right panel*). The Kv1.3 current amplitude increased modestly after 48 h of activation through the T cell receptor with anti-CD3 antibody, but the 500–600 Kv1.3 channels/cell in these activated cells only produced faint ShK-F6CA staining (Fig. 5, *middle right panels*). As with rat cells, repeatedly stimulated human T cells specific for the vaccine antigen TT expressed large Kv1.3 currents (~1500 channels/cell) and exhibited reproducible ShK-F6CA staining 48 h after the ninth round of antigenic stimulation (Fig. 5, *bottom right panels*). Similar results were obtained with human myelin-specific T cells that had been repeatedly stimulated with MBP (data not shown). ShK-F6CA staining thus clearly differentiates chronically activated rat and human T cells with ~1500–2000 Kv1.3 channels/cell from lymphocytes with channel numbers below 600/cell.

ShK-F6CA Staining Parallels Up-regulation of Kv1.3 Expression during Antigenic Activation of Rat T Cells—To study the time course of Kv1.3 up-regulation in chronically activated cells, we measured Kv1.3 expression and ShK-F6CA staining in a long term MBP-specific encephalitogenic rat T cell line, PAS, before and at various times after activation with MBP. PAS cells that had been "rested" in TCGF medium for 5 days after the last antigenic stimulation expressed small Kv1.3 currents and increased Kv1.3 expression dramatically after MBP stimulation, peaking in about 15 h (Fig. 6*A*). The channel levels remained elevated for the next 48 h during which time PAS cells are at their peak of encephalitogenicity (11, 32). Following the addition of TCGF at the 48th h, Kv1.3 levels progressively declined to a base line of <500 channels/cell on day 8 paralleling the decrease in encephalitogenicity (11, 32). Representative Kv1.3 currents measured 3, 4, 6, and 7 days post-activation are superimposed in Fig. 6*B* and demonstrate this time-dependent reduction in channel expression from the peak reached on days 1–3. The other K^+ channel in these cells, *IKCa1*, remained at ~100 channels/cell throughout the activation cycle (data not shown).

ShK-F6CA staining intensity changed in parallel with the up- and down-regulation of functional Kv1.3 expression. On days 1 to 4 post-stimulation, cells with 1000–2000 Kv1.3 channels/cell (Fig. 6*A*) stained brightly with ShK-F6CA (Fig. 6*C*, *top panels*). Weak ShK-F6CA staining was observed on day 6 (Fig. 6*C*, *lower left panel*) when the cells express ~750 channels/cell, whereas staining was undetectable on day 7 when the cells express <500 channels/cell (Fig. 6*C*, *lower right panel*). These results indicate that the increase and decrease of Kv1.3 functional expression during the activation process are due to changes in the number of Kv1.3 tetramers present in the cell membrane, each tetramer binding one molecule of ShK-F6CA. Our data also establish the detection limit for ShK-F6CA staining at about 600 Kv1.3 channels/cell (Fig. 6*C*). By using this cut off, it is feasible to distinguish encephalitogenic Kv1.3^{high} myelin antigen-activated T cells from non-encephalitogenic Kv1.3^{low} rested myelin-reactive cells or normal lymphocytes.

Calcium and Protein Kinase C (PKC)-dependent Pathways Are Required for Kv1.3 Up-regulation—Stimulation through the T cell receptor activates two major signaling pathways, the first involving calcium and the second PKC (34–36). We used a pharmacological approach to determine whether one or both these pathways were responsible for the up-regulation of Kv1.3 channel expression following antigenic activation of PAS T cells. Kv1.3 current amplitudes and ShK-F6CA staining, 20–30 h after MBP activation and in the presence or absence of pharmacological agents, are shown in Fig. 7, *A* and *B*, respectively. MBP activation of PAS cells augmented functional Kv1.3 expression to a maximum of 2000 ± 121 channels/cell (S.E., $n = 62$ cells) from a base line of 408 ± 39 Kv1.3 channels/cell ($n = 19$ cells, $p < 0.001$) in cells resting in TCGF medium for 4 days. ShK-F6CA staining also increased corresponding to the increased Kv1.3 level. CsA (100 nM), at a concentration that completely inhibits calcium-calcineurin-dependent nuclear factor of activated T cells activation, and staurosporine (10 nM), a PKC inhibitor, significantly suppressed MBP-induced Kv1.3 up-regulation (CsA, 1174 ± 115 channels/cell, $n = 23$, $p = 0.003$; staurosporine, 1062 ± 133 channels/cell, $n = 13$, $p < 0.001$) and decreased the intensity of ShK-F6CA staining. We could not study the effect of simultaneous inhibition of both pathways because cells exposed concurrently to CsA and staurosporine died. Neither agent had a direct effect on Kv1.3 channels as demonstrated by an absence of effect when either CsA or staurosporine was applied in the bath during whole-cell patch clamp (data not shown). Blockade of Kv1.3 channels by 100 nM MgTX during activation also suppressed MBP-triggered augmentation of functional Kv1.3 expression (MgTX, 637 ± 124 channels/cell, $n = 19$, $p < 0.001$) and ShK-F6CA staining intensity. Reduced Kv1.3 numbers in these cells were not due to direct blockade of the channel by residual MgTX, because the cells were washed extensively before patching and staining, and we had ascertained in other experiments that this procedure was sufficient to wash out MgTX (data not shown). ShK or ShK-F6CA could not be used for this experiment because it was not possible to wash them out completely (5). Suppression of Kv1.3 up-regulation by MgTX is probably due to attenuation of the calcium-signaling cascade upstream to the point of interruption by CsA (4, 37). Taken together, these results indicate that Kv1.3 up-regulation requires the activation of both the calcium- and PKC-dependent signaling pathways.

DISCUSSION

T cells expressing unusually high levels of the Kv1.3 channel have recently been implicated in an animal model for MS (7), and we now describe a tool for the detection of Kv1.3^{high} cells in tissues to facilitate the study of these cells in MS pathogenesis. We attached F6CA to ShK-Arg^1 so as not to interfere with the ShK-Kv1.3-interacting surface, and this fluorescent toxin, ShK-F6CA, exhibited low picomolar affinity for Kv1.3 and >80-fold selectivity for Kv1.3 over closely related K_V channels. When used in flow cytometry, the 1:1 stoichiometry of interaction between ShK-F6CA and Kv1.3 resulted in a small but

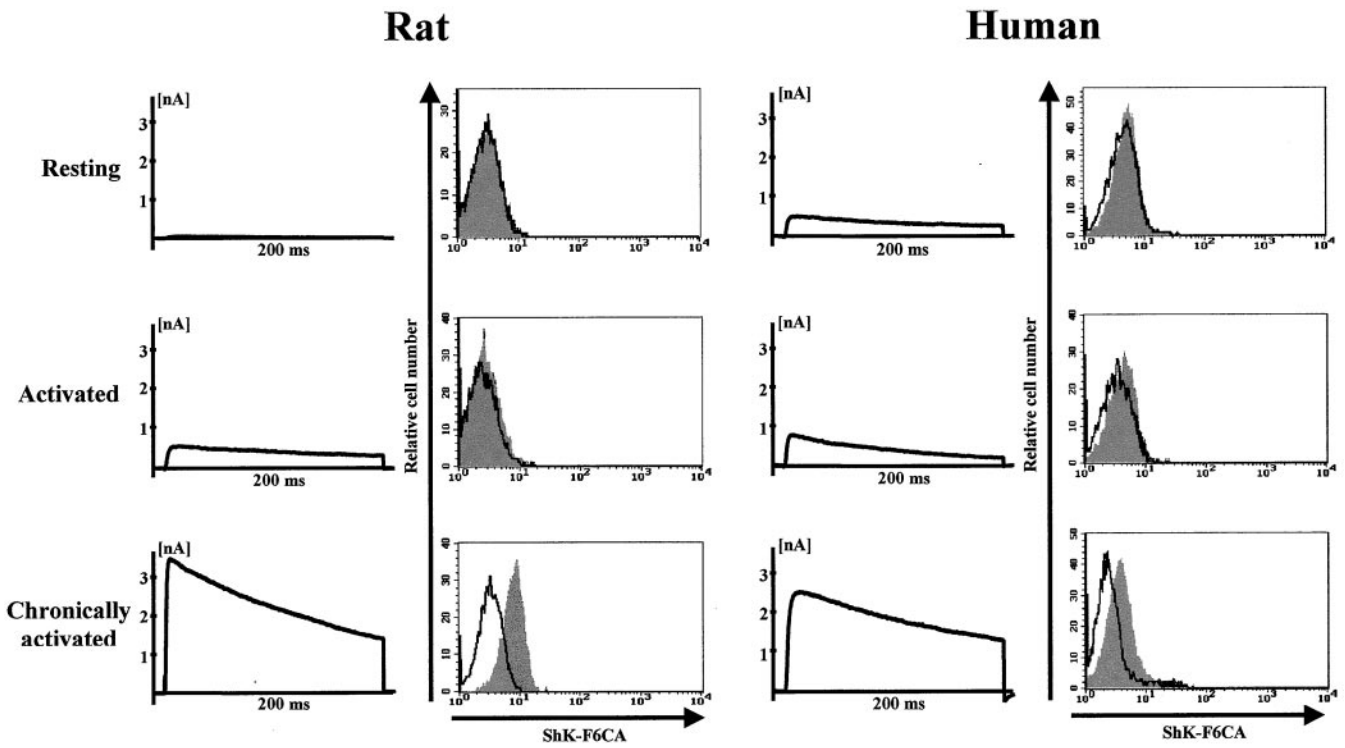

FIG. 5. **ShK-F6CA only stains rat and human T lymphocytes expressing high numbers of Kv1.3 channels.** Kv1.3 currents expressed by three populations (resting, one-time activated, and chronically activated) of rat or human T cells. Flow cytometry profiles of the same rat or human T cell populations unstained (*black lines*) or stained with 10 nM ShK-F6CA (*shaded*).

reproducible signal in flow cytometry with a detection limit of ~600 channels per cell. Repeatedly activated rat and human memory T cell lines with channel numbers above the detection limit were clearly identified by ShK-F6CA staining, whereas resting or acutely activated lymphocytes with lower Kv1.3 channel expression were below the detection limit using flow cytometry. ShK-F6CA might therefore have use in the rapid identification of Kv1.3^{high} cells in normal and diseased tissues.

Myelin-specific T cells in MS patients are reported to exhibit properties of memory T cells (38–40), and such cells could potentially contribute to the pathogenesis in MS because they traffic directly to inflamed tissues and release copious amounts of inflammatory cytokines such as interferon-γ and tumor necrosis factor-α. Kv1.3^{high} expression may therefore be a functional marker for such pathogenic myelin-reactive memory cells. In keeping with this idea, we have reported previously (7) that MBP-specific rat memory T cells express higher levels of Kv1.3 channels than naive rat T cells and induce severe EAE following adoptive transfer into rats. The level of Kv1.3 expression in these rat MBP-specific memory T cell lines correlates with their encephalitogenic potential, further highlighting the possible role of Kv1.3 in EAE pathogenesis. Furthermore, in rats that have received Kv1.3^{high} encephalitogenic T cells Kv1.3 blockade *in vivo* significantly ameliorates adoptive EAE (7, 12). If pathogenic myelin-specific T cells in MS patients exhibit the Kv1.3^{high} channel phenotype found in their encephalitogenic rat T cell counterparts, it may be feasible to identify such cells using ShK-F6CA staining. One could imagine an assay in which T cells freshly isolated from the blood of MS patients are activated by a mixture of myelin antigens for 48 h, stained with ShK-F6CA and memory T cell markers, and subjected to flow cytometry. The detection of increased numbers of myelin antigen-activated ShK-F6CA^{+} memory T lymphocytes in MS patients might have clinical utility as a surrogate marker for disease activity.

Generalization of this approach of tagging polypeptide inhibitors of ion channels with fluorophores could lead to the development of novel reagents for flow cytometry. For example, primary acute myeloid leukemia and hematopoietic cell lines aberrantly express increased levels of HERG K^{+} channels, which have been suggested to regulate proliferation in these cells (41, 42). A fluorophore-labeled version of the selective HERG channel blocker BeKm-1 (43) might be a valuable tool to detect these tumor cells. A limitation of our approach is the sensitivity of detection; cells with less than ~600 channels per cell are invisible. The use of other fluorophores to label the toxin or more sensitive methods may enable detection to the level of individual channels.

We investigated the intracellular signaling pathways that lead to up-regulated Kv1.3 expression in chronically activated memory T cells, using a combination of whole-cell recording and ShK-F6CA. The parallel increase in Kv1.3 channel numbers and ShK-F6CA staining indicates that enhanced functional Kv1.3 expression is the consequence of increased Kv1.3 tetramers in the membrane. Our results validate the utility of using fluorescently tagged Kv1.3 to investigate channel up-regulation and help to define a calcium- and PKC-dependent pathway that leads to the high level of expression seen in memory T cells. Naive T cells differ from memory T cells by augmenting IKCa1 levels upon activation instead of Kv1.3 (6, 7). IKCa1 up-regulation in these cells is mediated by PKC-, AP1-, and Ikaros-2-dependent transcription with no involvement of the calcium-signaling pathway (6). Functional consequences resulting from these differences in K^{+} channel expression are evident in the responsiveness of naive and memory cells to specific IKCa1 and Kv1.3 inhibitors. IKCa1 but not Kv1.3 blockers suppress the activation of lymphocytes with up-regulated IKCa1 levels, whereas Kv1.3 but not IKCa1 inhibitors suppress the activation of Kv1.3^{high} memory cells (7). The increased tendency of lymphocytes with up-regulated IKCa1 to exhibit oscillatory calcium signals (44, 45) also points to a potential functional difference with Kv1.3^{high} cells. Up-

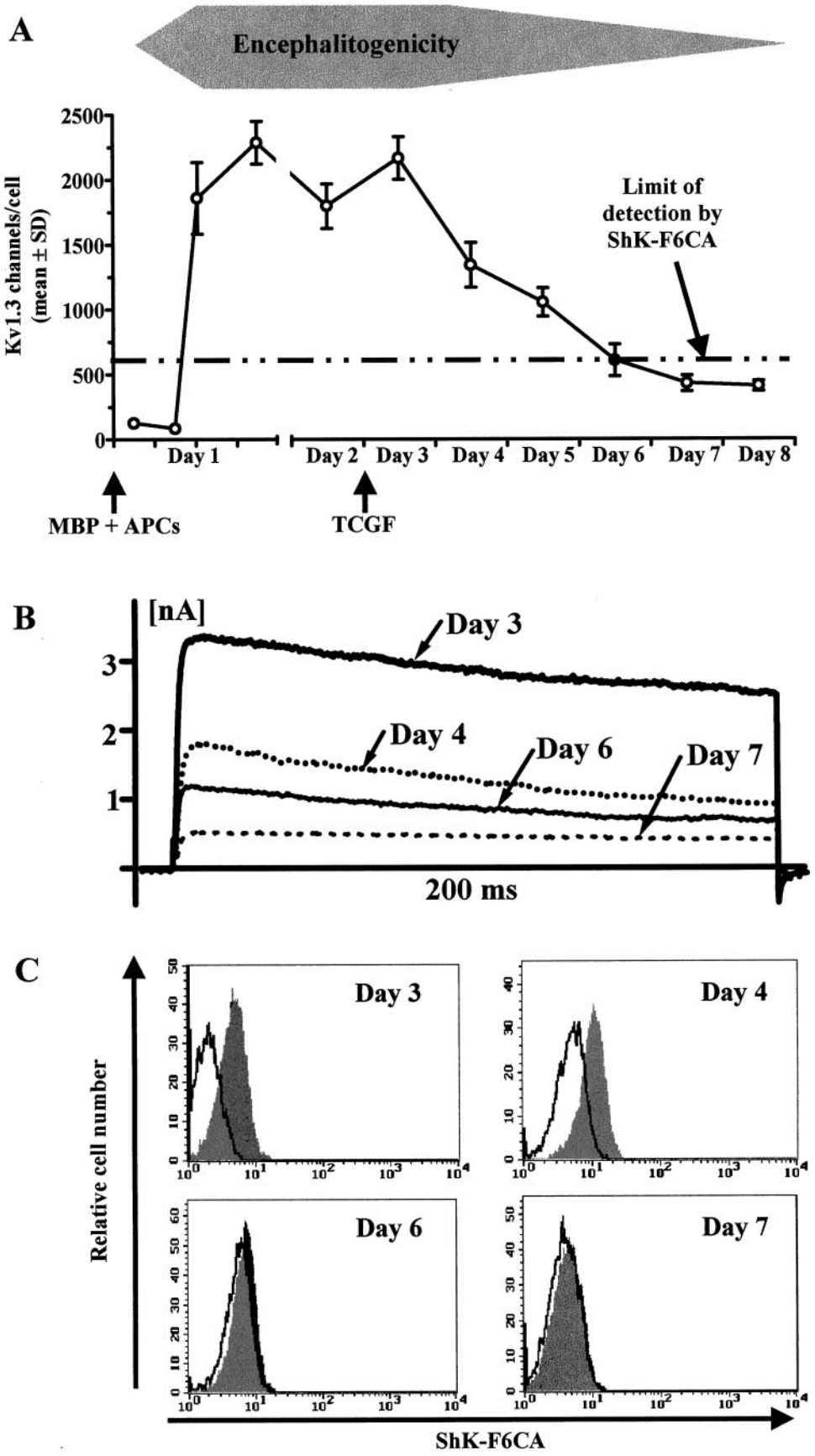

FIG. 6. **ShK-F6CA staining intensity correlates with up- and down-regulation of Kv1.3 channels by encephalitogenic rat memory T cells.** *A*, average numbers of Kv1.3 channels/cell (n = 13 to 29 ± S.E.) are plotted *versus* time after antigen-induced activation of PAS T cells. *Arrows below* the plot mark the time of stimulation with MBP and of addition of TCGF. *B*, representative Kv1.3 currents expressed by PAS T cells on days 3, 4, 6, and 7 after activation. *C*, flow cytometry profiles (unstained controls: *black lines*; cells stained with ShK-F6CA: *shaded*) of PAS T cells acquired on days 3, 4, 6, and 7 after antigen-induced activation.

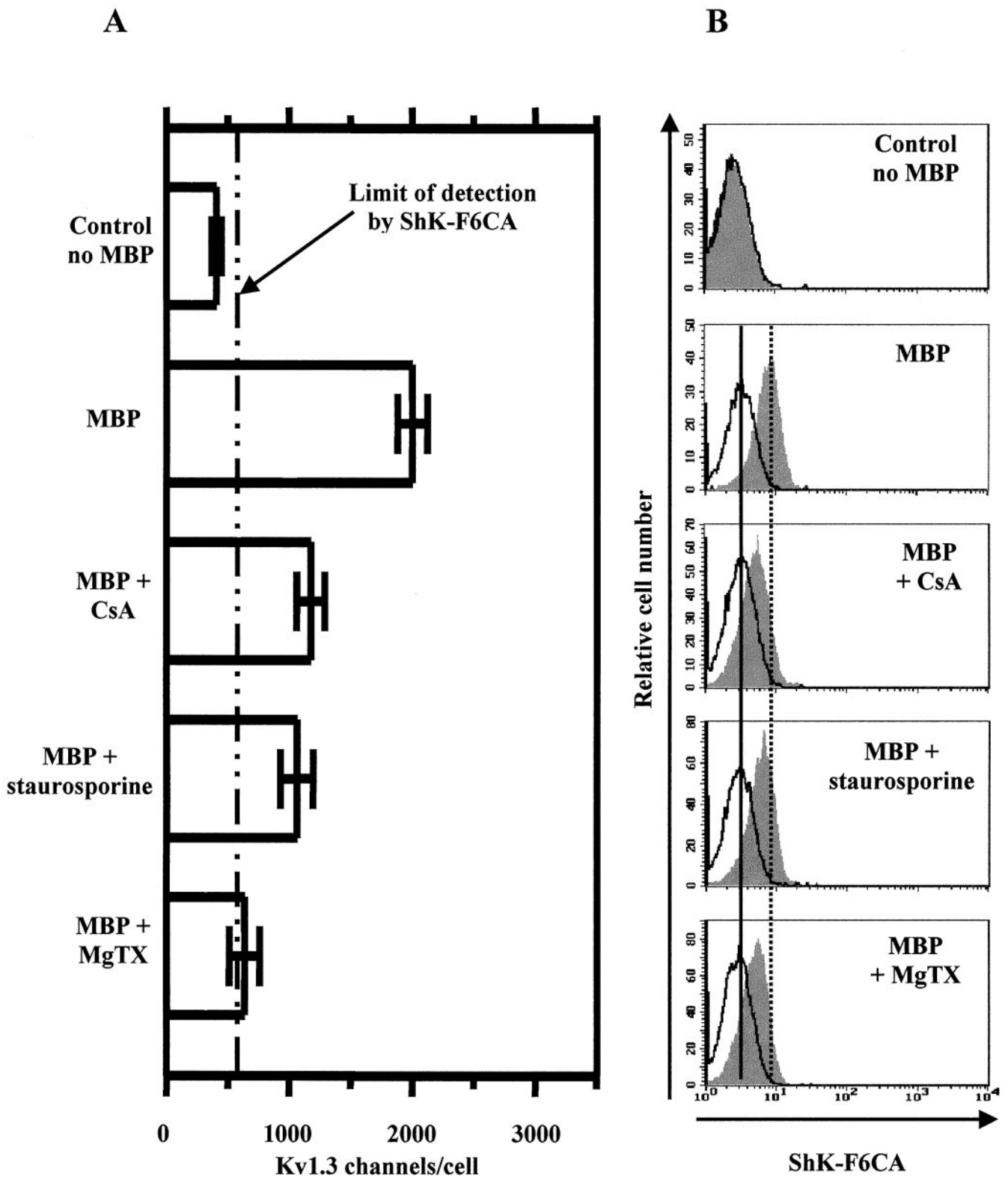

FIG. 7. **Essential role of the pathways leading to the activation of nuclear factor of activated T cells in the up-regulation of Kv1.3 channels by rat T cells.** *A*, average numbers of Kv1.3 channels/cell (n = 13 to 62 ± S.E.) are shown for each culture condition. PAS T cells were stimulated with MBP in the presence of either 100 nM CsA, 10 nM staurosporine, or 100 nM MgTX and were cultured for 20–30 h before determination of Kv1.3 channel numbers by patch clamp. The *dashed line* indicates the limit of detection of Kv1.3 channels by ShK-F6CA (~600 channels/cell). *B*, PAS T cells stimulated in the presence of the pharmacological agents listed in *A* and stained with 10 nM ShK-F6CA 20–30 h later (*shaded*; unstained controls are shown as *black lines*).

regulated Kv1.3 expression in memory cells may promote cell adhesion and migration via the reported interaction between Kv1.3 and β integrins (46). The channel may also participate in signaling at the immunological synapse through possible interactions with PKC and p56^{lck} (47). Through the use of tools such as ShK-F6CA, it may be feasible to visualize fluorescently tagged Kv1.3 channels at the immunological synapse during antigen presentation. Fluorescent probes that directly mark

functional channels in the membrane may therefore find utility as diagnostic tools that can distinguish between subsets of cells with varying channel phenotypes and as experimental tools to locate channels within the cell during locomotion or immunological synapse formation.

Acknowledgments—We thank Dr. Fang-yao Stephen Hou for expert advice on flow cytometry and Dr. Evelyne Béraud for the generous gift of the PAS T cell line.

REFERENCES

1. DeCoursey, T. E., Chandy, K. G., Gupta, S., and Cahalan, M. D. (1984) *Nature* **307,** 465–468
2. Chandy, K. G., DeCoursey, T. E., Cahalan, M. D., McLaughlin, C., and Gupta, S. (1984) *J. Exp. Med.* **160,** 369–385
3. Price, M., Lee, S. C., and Deutsch, C. (1989) *Proc. Natl. Acad. Sci. U. S. A.* **86,** 10171–10175
4. Koo, G. C., Blake, J. T., Talento, A., Nguyen, M., Lin, S., Sirotina, A., Shah, K., Mulvany, K., Hora, D., Jr., Cunningham, P., Wunderler, D. L., McManus, O. B., Slaughter, R., Bugianesi, R., Felix, J., Garcia, M., Williamson, J., Kaczorowski, G., Sigal, N. H., Springer, M. S., and Feeney, W. (1997) *J. Immunol.* **158,** 5120–5128
5. Kalman, K., Pennington, M. W., Lanigan, M. D., Nguyen, A., Rauer, H., Mahnir, V., Paschetto, K., Kem, W. R., Grissmer, S., Gutman, G. A., Christian, E. P., Cahalan, M. D., Norton, R. S., and Chandy, K. G. (1998) *J. Biol. Chem.* **273,** 32697–32707
6. Ghanshani, S., Wulff, H., Miller, M. J., Rohm, H., Neben, A., Gutman, G. A., Cahalan, M. D., and Chandy, K. G. (2000) *J. Biol. Chem.* **275,** 37137–37149
7. Beeton, C., Wulff, H., Barbaria, J., Clot-Faybesse, O., Pennington, M., Bernard, D., Cahalan, M. D., Chandy, K. G., and Beraud, E. (2001) *Proc. Natl. Acad. Sci. U. S. A.* **98,** 13942–13947
8. Hohlfeld, R., and Wekerle, H. (2001) *Curr. Opin. Neurol.* **14,** 299–304
9. Steinman, L. (2001) *Nat. Immunol.* **2,** 762–764
10. O'Connor, K., Bar-Or, A., and Hafler, D. A. (2001) *J. Clin. Immunol.* **21,** 81–92
11. Strauss, U., Schubert, R., Jung, S., and Mix, E. (1998) *Receptors Channels* **6,** 73–87
12. Beeton, C., Barbaria, J., Giraud, P., Devaux, J., Benoliel, A., Gola, M., Sabatier, J., Bernard, D., Crest, M., and Beraud, E. (2001) *J. Immunol.* **166,** 936–944
13. Fadool, D. A., Holmes, T. C., Berman, K., Dagan, D., and Levitan, I. B. (1997) *J. Neurophysiol.* **78,** 1563–1573
14. Darbon, H., and Angelides, K. J. (1984) *J. Biol. Chem.* **259,** 6074–6084
15. Joe, E. H., and Angelides, K. J. (1993) *J. Neurosci.* **13,** 2993–3005
16. Jones, O. T., Kunze, D. L., and Angelides, K. J. (1989) *Science* **244,** 1189–1193
17. Benke, T. A., Jones, O. T., Collingridge, G. L., and Angelides, K. J. (1993) *Proc. Natl. Acad. Sci. U. S. A.* **90,** 7819–7823
18. Pragl, B., Koschak, A., Trieb, M., Obermair, G., Kaufmann, W. A., Gerster, U., Blanc, E., Hahn, C., Prinz, H., Schutz, G., Darbon, H., Gruber, H. J., and Knaus, H. G. (2002) *Bioconjugate Chem.* **13,** 416–425
19. Freudenthaler, G., Axmann, M., Schindler, H., Pragl, B., Knaus, H. G., and Schutz, G. J. (2002) *Histochem. Cell Biol.* **117,** 197–202
20. Sands, S. B., Lewis, R. S., and Cahalan, M. D. (1989) *J. Gen. Physiol.* **93,** 1061–1074
21. Garcia, M. L., Garcia-Calvo, M., Hidalgo, P., Lee, A., and MacKinnon, R. (1994) *Biochemistry* **33,** 6834–6839
22. Aiyar, J., Withka, J. M., Rizzi, J. P., Singleton, D. H., Andrews, G. C., Lin, W., Boyd, J., Hanson, D. C., Simon, M., Dethlefs, B., Lee, C.-L., Hall, J. E., Gutman, G. A., and Chandy, K. G. (1995) *Neuron* **15,** 1169–1181
23. Pennington, M., Byrnes, M., Zaydenberg, I., Khaytin, I., de Chastonay, J., Krafte, D., Hill, R., Mahnir, V., Volberg, W., Gorczyca, W., and Kem, W. (1995) *Int. J. Pept. Protein Res.* **346,** 354–358
24. Chandy, K. G., Cahalan, M. D., Pennington, M., Norton, R. S., Wulff, H., and Gutman, G. A. (2001) *Toxicon* **39,** 1269–1276
25. Rauer, H., Pennington, M., Cahalan, M., and Chandy, K. G. (1999) *J. Biol. Chem.* **274,** 21885–21892
26. Tudor, J. E., Pallaghy, P. K., Pennington, M. W., and Norton, R. S. (1996) *Nat. Struct. Biol.* **3,** 317–320
27. Norton, R. S., Pallaghy, P. K., Baell, J. B., Wright, C. E., Lew, M. J., and Angus, J. A. (1999) *Drug Dev. Res.* **46,** 206–218
28. Lanigan, M. D., Kalman, K., Lefievre, Y., Pennington, M. W., Chandy, K. G., and Norton, R. S. (2002) *Biochemistry* **41,** 11963–11971
29. King, D. S., Fields, C. G., and Fields, G. B. (1990) *Int. J. Pept. Protein Res.* **36,** 255–266
30. Grissmer, S., Nguyen, A. N., Aiyar, J., Hanson, D. C., Mather, R. J., Gutman, G. A., Karmilowicz, M. J., Auperin, D. D., and Chandy, K. G. (1994) *Mol. Pharmacol.* **45,** 1227–1234
31. Bardien-Kruger, S., Wulff, H., Arieff, Z., Brink, P., Chandy, K. G., and Corfield, V. (2002) *Eur. J. Hum. Genet.* **10,** 36–43
32. Beraud, E., Balzano, C., Zamora, A. J., Varriale, S., Bernard, D., and Ben-Nun, A. (1993) *J. Neuroimmunol.* **47,** 41–53
33. Wulff, H., Miller, M. J., Haensel, W., Grissmer, S., Cahalan, M. D., and Chandy, K. G. (2000) *Proc. Natl. Acad. Sci. U. S. A.* **97,** 8151–8156
34. Lewis, R. S. (2001) *Annu. Rev. Immunol.* **19,** 497–521
35. Isakov, N., and Altman, A. (2002) *Annu. Rev. Immunol.* **20,** 761–794
36. Arendt, C. W., Albrecht, B., Soos, T. J., and Littman, D. R. (2002) *Curr. Opin. Immunol.* **14,** 323–330
37. Lin, C. S., Boltz, R. C., Blake, J. T., Nguyen, M., Talento, A., Fischer, P. A., Springer, M. S., Sigal, N. H., Slaughter, R. S., Garcia, M. L., Kaczorowski, G., and Koo, G. (1993) *J. Exp. Med.* **177,** 637–645
38. Lovett-Racke, A. E., Trotter, J. L., Lauber, J., Perrin, P. J., June, C. H., and Racke, M. K. (1998) *J. Clin. Invest.* **101,** 725–730
39. Scholz, C., Anderson, D. E., Freeman, G. J., and Hafler, D. A. (1998) *J. Immunol.* **160,** 1532–1538
40. Markovic-Plese, S., Cortese, I., Wandinger, K. P., McFarland, H. F., and Martin, R. (2001) *J. Clin. Invest.* **108,** 1185–1194
41. Smith, G. A., Tsui, H. W., Newell, E. W., Jiang, X., Zhu, X. P., Tsui, F. W., and Schlichter, L. C. (2002) *J. Biol. Chem.* **277,** 18528–18534
42. Pillozzi, S., Brizzi, M. F., Crociani, O., Cherubini, A., Guasti, L., Bartolozzi, B., Becchetti, A., Wanke, E., Bernabei, P. A., Olivotto, M., Pegoraro, L., and Arcangeli, A. (2002) *Leukemia* (*Baltimore*) **16,** 1791–1798
43. Korolkova, Y. V., Kozlov, S. A., Lipkin, A. V., Pluzhnikov, K. A., Hadley, J. K., Filippov, A. K., Brown, D. A., Angelo, K., Strobaek, D., Jespersen, T., Olesen, S. P., Jensen, B. S., and Griskin, E. V. (2001) *J. Biol. Chem.* **276,** 9868–9876
44. Hess, S. D., Oortgiesen, M., and Cahalan, M. D. (1993) *J. Immunol.* **150,** 2620–2633
45. Verheugen, J. A., Le Deist, F., Devignot, V., and Korn, H. (1997) *Cell Calcium* **21,** 1–17
46. Levite, M., Cahalon, L., Peretz, A., Hershkoviz, R., Sobko, A., Ariel, A., Desai, R., Attali, B., and Lider, O. (2000) *J. Exp. Med.* **191,** 1167–1176
47. Cahalan, M. D., Wulff, H., and Chandy, K. G. (2001) *J. Clin. Immunol.* **21,** 235–252